Scale-Dependent Statistical Geometry in Two-Dimensional Flow

Sophia T. Merrifield, Douglas H. Kelley, and Nicholas T. Ouellette*

Department of Mechanical Engineering, Yale University, New Haven, Connecticut 06520, USA

(Received 25 March 2010; published 21 June 2010)

By studying the shape dynamics of three-particle clusters, we investigate the statistical geometry of a spatiotemporally chaotic experimental quasi-two-dimensional flow. We show that when shape and size are appropriately decoupled, these Lagrangian triangles assume statistically stationary shape distributions that depend on the flow scale, with smaller scales favoring more distorted triangles. These preferred shapes are not due to trapping by Eulerian flow structures. Since our flow does not have developed turbulent cascades, our results suggest that more careful work is required to understand the specific effects of turbulence on the advection of Lagrangian clusters.

DOI: 10.1103/PhysRevLett.104.254501 PACS numbers: 47.27.T−, 47.27.De, 47.52.+j

Accurately modeling the transport of scalar fields by complex flows has been a tremendous challenge, since the scalar displays highly anomalous scaling. The scalar field retains its intermittency even when the advecting flow field is not itself intermittent [1,2], as is thought to be the case, for example, for the inverse cascade in two-dimensional (2D) turbulence [3]. Recent breakthroughs in the mathematical description of scalar transport have succeeded in tying scalar intermittency to the multipoint Lagrangian dynamics of the flow via the phenomenology of ''zero modes'' [3–9]. A key quantity to consider in Lagrangian dynamics is the evolution of material volumes in the flow. Such volumes (or areas in 2D flow) can in turn be parametrized by clusters of fluid elements that evolve with the flow [3,10,11]. Both experiments [12] and simulations [11,13] have shown that Lagrangian clusters tend to assume statistically stationary shape distributions in turbulence.

A minimum of three fluid elements is required to parametrize a material area, the highest-dimensional structure in 2D flow. Such Lagrangian triangles have been studied previously in 2D in kinematic simulations [14] and experiments [15]. Both studies found similar results: under the action of the flow, triangles distorted from initially symmetric shapes, eventually reaching the uncorrelated random limit after long times. In both cases, and in related work in three-dimensional turbulence [11–13], this distortion was presumed to be due to the turbulence, particularly since the growth of the clusters appeared to follow expected turbulent scaling laws [11,13] and the time scale of the cluster distortion could be explained by Kolmogorov-type scaling arguments [12]. But since purely random fields without turbulent dynamics can lead to complex scalar advection [1,2], unsteady but nonturbulent flows may also drive nontrivial shape distortion.

In this Letter, we study the Lagrangian evolution of triplets of fluid elements in a quasi-2D flow that is unsteady and spatiotemporally chaotic, but not turbulent: we see no energy or enstrophy cascades and no inertial subranges [16]. Since our experimental apparatus and field of view are very large, we can follow the triangles for unusually long times. Surprisingly, we observe the same type of shape distortion as was previously found for turbulent flows. We also find that the size and shape of the triangles are strongly coupled: each length scale of the flow shows a statistically stationary distribution of triangle shapes, but the distributions change as a function of scale. We find no direct connection between the shape distributions and the mean Eulerian structure of the flow field on corresponding length scales. The shapes we see must therefore be the result of the flow dynamics, even without energy or enstrophy cascades. Our results indicate that turbulence is not a prerequisite for complex statistical geometry, and suggest that multiscale shape dynamics may be much more generic in nonlinear systems than has been previously recognized.

We drive quasi-2D flow electromagnetically in a thin layer of conducting fluid in a flow cell that has been described in detail elsewhere [16]. Briefly, we place a layer of salt water (16% NaCl by mass) roughly 4 mm deep above an array of strong permanent magnets arranged in a square lattice of alternating polarity. The magnets are placed with a center-to-center separation of 2.54 cm, and this spacing sets the forcing length scale L_f. Our flow cell is quite large, with a total driven area of 86×86 cm^2, of which we typically study the central 31×23 cm^2 region so that the effect of the sidewalls is negligible. The salt water is separated from the magnets by a thin glass plate, which is coated with a layer of hydrophobic wax in order to reduce bottom drag. By driving electric current (up to roughly 1 A) laterally through the electrolyte, we generate Lorentz forces that set the fluid into motion [17–20]. We characterize the nondimensional strength of the forcing with the Reynolds number $\mathrm{Re} = u' L_f/\nu$, where u' is the in-plane root-mean-square velocity and ν is the kinematic viscosity. We estimate the time scale of the forcing to be $T_L = L_f/u'$. We measure the dynamics of the flow by seeding it with 51 μm fluorescent polystyrene particles that follow the flow [20]; we track their motion at a rate of 25 Hz and with a precision of roughly 13 μm using a multiframe predictive tracking algorithm [21]. The par-

ticles lie at the interface between the salt water and a less dense fresh water layer (of similar depth). Because of the miscibility of the layers, surface-tension-driven interactions among the particles [22] are negligible. Since we follow up to 35 000 particles per frame, we can construct high-resolution velocity fields at each time step. We then project the measured velocity fields onto a basis of stream-function eigenmodes [16], which both filters noise from the data and ensures that the fields are robustly 2D and incompressible in the plane. We note that even though our particle loading is high, the tracers are typically at least 17 diameters apart; hydrodynamic interactions among the particles are therefore negligible.

In this work, we are concerned with triangle shape rather than position or orientation; as the shape of a triangle has 2 degrees of freedom, we require two independent parameters to describe each three-particle configuration. It has become common to follow the lead of Refs. [23,24] and define vectors $\boldsymbol{\rho}_1 \equiv (\boldsymbol{r}_2 - \boldsymbol{r}_1)/\sqrt{2}$ and $\boldsymbol{\rho}_2 \equiv (2\boldsymbol{r}_3 - \boldsymbol{r}_2 - \boldsymbol{r}_1)/\sqrt{6}$, where $\boldsymbol{r}_n$ is the position of the nth triangle vertex, to describe the reduced dynamics of triangles [3,7,10,11,14,15]. The quantities $\chi \equiv (1/2) \times \arctan[2\boldsymbol{\rho}_1 \cdot \boldsymbol{\rho}_2/(\rho_2^2 - \rho_1^2)]$ and $w \equiv 2|\boldsymbol{\rho}_1 \times \boldsymbol{\rho}_2|/(\rho_1^2 + \rho_2^2)$ can then be defined to characterize the triangle shape [3,11,14,15]. This approach is useful in that it is straightforward to generalize to clusters with more points (such as four-point Lagrangian "tetrads" [10]); for all but the simplest shapes, however, χ and w do not have clear geometric meanings [15]. We prefer, therefore, to work with a more straightforward shape parametrization. Let us label the side lengths of a triangle as Λ_1, Λ_2, and Λ_3, with $\Lambda_1 \geq \Lambda_2 \geq \Lambda_3$, and the internal angles as θ_1, θ_2, and θ_3, again with $\theta_1 \geq \theta_2 \geq \theta_3$. We describe the shape of a triangle with the largest internal angle θ_1, which tells us how obtuse the triangle is, and $\gamma \equiv \Lambda_3/\Lambda_2$, the ratio of the smallest side to the intermediate side, which tells us how close together the nearest two points are. We note that $\theta_1 \in [\pi/3, \pi]$ and $\gamma \in [0, 1]$. In Fig. 1, we show triangles at different points in this two-dimensional shape space.

In order to follow the evolution of triangles for long periods of time, we compute the trajectories of virtual Lagrangian points through our measured velocity fields using the same method as in Ref. [20]. As has been demonstrated previously in similar quasi-2D electromagnetically forced flows [17,18,20], our results are similar, though noisier, when using actual measured particle tracks. Of primary concern for this work, however, the measured trajectories tend to be short or broken, since we use a very high tracer seeding density, and therefore sample only the short-time behavior of the triangles. Long measured tracks may also be plagued by finite-volume biases [25]. Studying unbiased long-time statistics therefore requires a numerical approach like the one we use.

The energy spectrum of our flow shows no power-law scaling [16], suggesting that we have no turbulent cascades. The only well defined length scale in the flow is

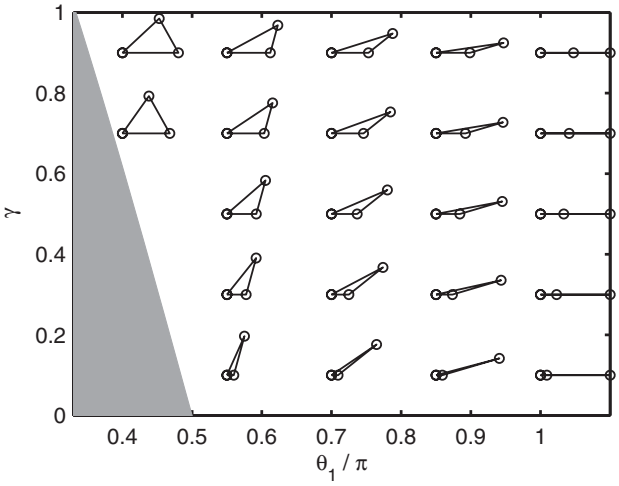

FIG. 1. Example triangle shapes in the 2D phase space spanned by γ and θ_1. Shapes in the gray region are not allowed.

therefore the forcing scale L_f. We might therefore expect that triangles should behave differently when they are large or small compared to L_f. In Fig. 2, we show the evolution of the mean shape for initially equilateral ($\theta_1 = \pi/3$, $\gamma = 1$) triangles with four different initial sizes Λ_0: $\Lambda_0 = L_f/20$, $\Lambda_0 = L_f/2$, $\Lambda_0 = L_f$, and $\Lambda_0 = 2L_f$. Data are shown for Re = 185; our results are similar for other Reynolds numbers above the transition to spatiotemporal chaos [19]. At long times, all four sets of triangles approach the same limits. The final values can be found by computing the mean shapes of triplets of points drawn from an isotropic uniform distribution, as has been shown previously [11]. We find a nearly identical long-time limit by simulating triangles evolving via simple Brownian dynamics. Strikingly, however, the two experimental curves for triangles with their initial sizes smaller than the forcing length L_f overshoot the long-time values before subsequently relaxing to the random limit. The trends are perhaps more evident in Fig. 2(c), where we plot the evolution of the triangles in the 2D shape space spanned by θ_1 and γ. This type of behavior has been observed previously [11,14,15], but typically has been ascribed to the action of turbulence. Here, however, we have no energy or enstrophy cascades and no inertial subranges [16].

If turbulence is not driving the initial strong distortion of the triangle shapes and their subsequent relaxation to the random limit, there must be an alternative explanation. We argue that the overshoots result from a failure to decouple triangle *size* from triangle *shape*. Perhaps different flow scales have different preferred statistical geometries, and the resulting nonmonotonic triangle-evolution curves simply mark the passage of the triangles into different scale regimes. It is certainly true that the triangles grow at the same time as they change their shape; such rapid growth is generic in both turbulent [13,26] and chaotic flow [27]. The conflation of these two effects has been suggested as a contributing factor in the difficulty of observing

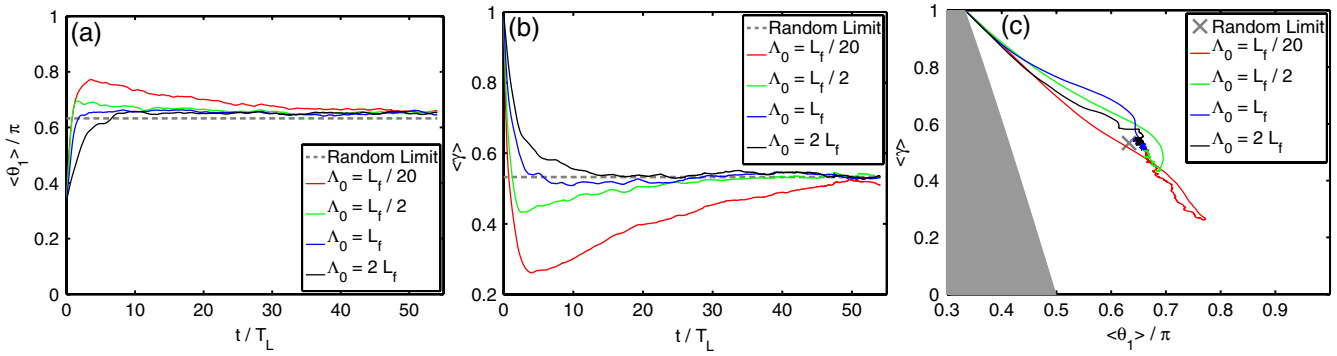

FIG. 2 (color online). (a) $\langle\theta_1\rangle$ and (b) $\langle\gamma\rangle$ (where $\langle\cdot\rangle$ denotes ensemble averaging) as a function of time for initially equilateral triangles of varying initial size Λ_0 at a Reynolds number of Re = 185. For triangles with $\Lambda_0 < L_f$, the shape factors overshoot their stationary values before relaxing to the random limit. In (c), the same data are plotted in the 2D shape phase space; as in Fig. 1, shapes in the gray region are not allowed.

Richardson pair dispersion in fully developed turbulence [18,28].

To test the hypothesis that the size of the triangles is affecting the shape distributions, we dynamically separated the shape distributions of triangles that grow at different rates as they evolve. We began with a population of equilateral triangles of initial side length $\Lambda_0 = L_f/20$. At each time step, we computed the mean shapes for triangles with sizes falling in one of five bins, ranging from triangles that remained the same size or shrank to triangles much larger than the forcing scale. The fraction of the total number of triangles in each bin is shown as a function of time in Fig. 3, giving an indication of how fast the population of triangles grows. Our results for the evolution of the largest internal angle for the triangles in each bin are shown in Fig. 4. Although there are large fluctuations in the long-time data for the smallest bins (since few triangles remain small after many forcing time scales), the trend is clear. The triangles in each size range assume statistically stationary shapes, but the chosen shape distribution varies with scale. In general, smaller triangles are more distorted. Figure 5 shows the same results in the 2D (θ_1, γ) space; again, although there are large fluctuations, it is clear that different scales show different statistical geometry.

It is natural to try to connect the observed shape distributions to differences in the flow structure at different scales. Khan, Pumir, and Vassilicos [14], for example, suggested that the spatial density of straining regions in their kinematic simulation (which they varied by changing the energy spectrum) modified the triangle shape distributions. We have shown that the spatial structure of the velocity field in our flow changes strongly as a function of scale [16]; in particular, regions of large enstrophy or strain become much more elongated at smaller scales [29]. It is therefore reasonable to suggest that the triangles may be caught in high-aspect-ratio Eulerian coherent structures that are then determining the triangle shapes. To address

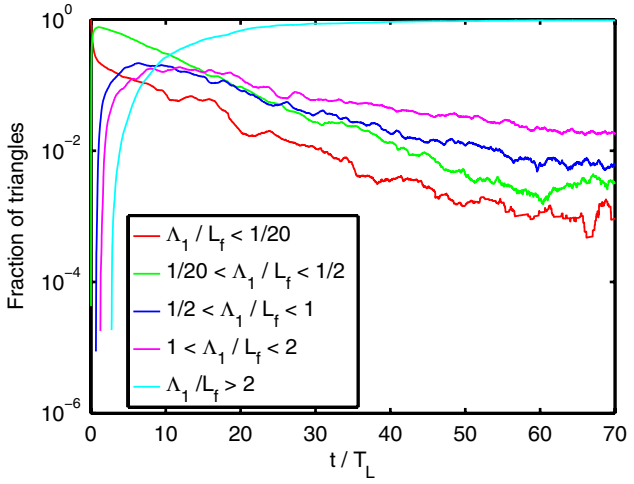

FIG. 3 (color online). Fraction of the total number of triangles for each of the indicated sizes as a function of time, plotted semilogarithmically. The triangles were initially equilateral with side lengths of $\Lambda_0 = L_f/20$. The number of triangles per size range falls off roughly exponentially with time, as is expected for a chaotic flow.

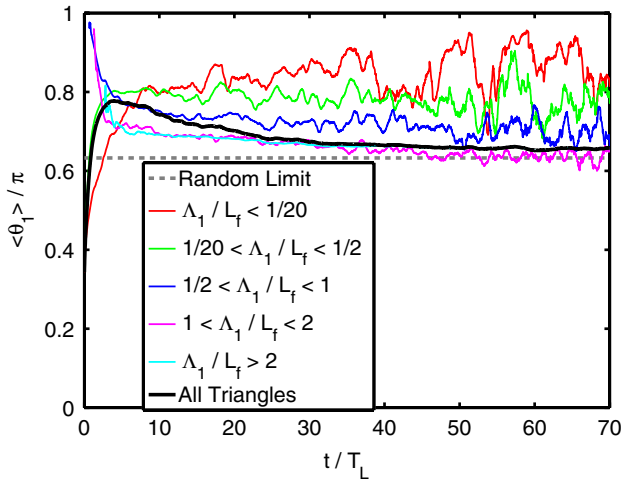

FIG. 4 (color online). $\langle\theta_1\rangle$ as a function of time for initially equilateral triangles with $\Lambda_0 = L_f/20$. Unlike in Fig. 2, we here separate the triangle growth from the evolution of the shape factors by binning the triangles based on their size as time evolves.

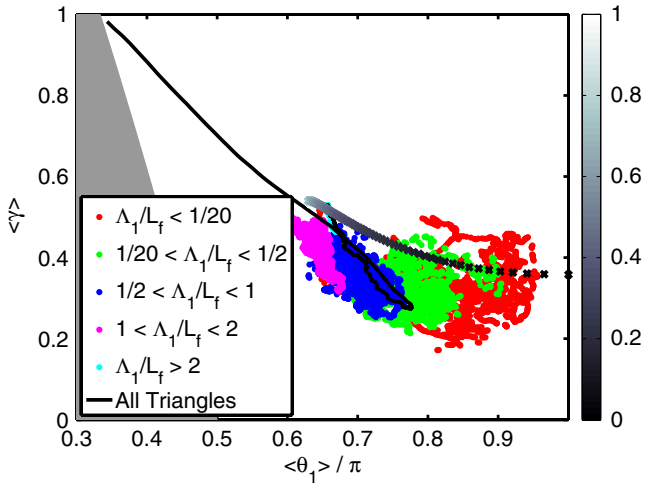

FIG. 5 (color online). Evolution of triangles binned as in Fig. 4 in the 2D shape phase space. Note that we have removed the initial transient evolution for each of the binned distributions. The crosses show confinement-limited shapes; the aspect ratio of the confinement box is given by the color bar.

this hypothesis, we used a Monte Carlo approach to compute the mean triangle shapes obtained from placing uniformly distributed points constrained to lie in ellipses of aspect ratios (defined as the ratio of the minor to the major axis) ranging from zero to one. The resulting mean shapes are shown in Fig. 5. While the final large-scale limit is close to the isotropic random limit, as shown before in Fig. 2(c), this type of confinement effect is clearly not responsible for the small-scale shape distributions. This result suggests a dynamical origin for the observed small-scale shape distributions rather than one connected to Eulerian coherent structures.

To summarize, we have studied the shape dynamics of Lagrangian triangles in a spatiotemporally chaotic flow. By following the triangles for very long times, we have shown that triangles—regardless of initial size—eventually assume a shape distribution close to that expected for randomly placed points. By appropriately decoupling shape and size, however, we have shown that each scale of the flow in fact shows a different preferred statistical geometry, with smaller scales favoring more distorted triangles. Our Monte Carlo simulations show that these preferred shape distributions are not due to the trapping of the triangles in coherent structures, since simple geometric confinement cannot produce the observed stationary shapes. Our results therefore point toward a dynamical explanation of triangle shape. Finally, we note again that we see results similar to those found before in turbulence, even though our flow is not turbulent and does not have energy or enstrophy cascades. More work is therefore needed to tease apart the detailed contributions of *turbulence* to the shape dynamics of Lagrangian clusters.

We acknowledge helpful conversations with W. Ellenbroek during the early stages of this project. This work was supported by the U.S. National Science Foundation under Grant No. DMR-0906245.

*nicholas.ouellette@yale.edu

[1] R. H. Kraichnan, Phys. Rev. Lett. **72**, 1016 (1994).
[2] R. H. Kraichnan, V. Yakhot, and S. Chen, Phys. Rev. Lett. **75**, 240 (1995).
[3] A. Celani and M. Vergassola, Phys. Rev. Lett. **86**, 424 (2001).
[4] M. Chertkov, G. Falkovich, I. Kolokolov, and V. Lebedev, Phys. Rev. E **52**, 4924 (1995).
[5] K. Gawędzki and A. Kupiainen, Phys. Rev. Lett. **75**, 3834 (1995).
[6] U. Frisch, A. Mazzino, and M. Vergassola, Phys. Rev. Lett. **80**, 5532 (1998).
[7] L. Mydlarski, A. Pumir, B. I. Shraiman, E. D. Siggia, and Z. Warhaft, Phys. Rev. Lett. **81**, 4373 (1998).
[8] B. I. Shraiman and E. D. Siggia, Nature (London) **405**, 639 (2000).
[9] G. Falkovich, K. Gawędzki, and M. Vergassola, Rev. Mod. Phys. **73**, 913 (2001).
[10] M. Chertkov, A. Pumir, and B. I. Shraiman, Phys. Fluids **11**, 2394 (1999).
[11] A. Pumir, B. I. Shraiman, and M. Chertkov, Phys. Rev. Lett. **85**, 5324 (2000).
[12] H. Xu, N. T. Ouellette, and E. Bodenschatz, New J. Phys. **10**, 013 012 (2008).
[13] L. Biferale, G. Boffetta, A. Celani, B. J. Devenish, A. Lanotte, and F. Toschi, Phys. Fluids **17**, 111 701 (2005).
[14] M. A. I. Khan, A. Pumir, and J. C. Vassilicos, Phys. Rev. E **68**, 026313 (2003).
[15] P. Castiglione and A. Pumir, Phys. Rev. E **64**, 056303 (2001).
[16] D. H. Kelley and N. T. Ouellette, arXiv:1004.4687.
[17] G. A. Voth, G. Haller, and J. P. Gollub, Phys. Rev. Lett. **88**, 254501 (2002).
[18] M. K. Rivera and R. E. Ecke, Phys. Rev. Lett. **95**, 194503 (2005).
[19] N. T. Ouellette and J. P. Gollub, Phys. Rev. Lett. **99**, 194502 (2007).
[20] N. T. Ouellette, P. J. J. O'Malley, and J. P. Gollub, Phys. Rev. Lett. **101**, 174504 (2008).
[21] N. T. Ouellette, H. Xu, and E. Bodenschatz, Exp. Fluids **40**, 301 (2006).
[22] D. Vella and L. Mahadevan, Am. J. Phys. **73**, 817 (2005).
[23] B. I. Shraiman and E. D. Siggia, Phys. Rev. E **57**, 2965 (1998).
[24] A. Pumir, Phys. Rev. E **57**, 2914 (1998).
[25] J. Berg, S. Ott, J. Mann, and B. Lüthi, Phys. Rev. E **80**, 026316 (2009).
[26] M. Bourgoin, N. T. Ouellette, H. Xu, J. Berg, and E. Bodenschatz, Science **311**, 835 (2006).
[27] T. H. Solomon, E. R. Weeks, and H. L. Swinney, Physica (Amsterdam) **76D**, 70 (1994).
[28] G. Boffetta and I. M. Sokolov, Phys. Rev. Lett. **88**, 094501 (2002).
[29] S. Chen, R. E. Ecke, G. L. Eyink, M. Rivera, M. Wan, and Z. Xiao, Phys. Rev. Lett. **96**, 084502 (2006).